

An improved maximum power point tracking method for photovoltaic systems

T. Tafticht, K. Agbossou*, M.L. Doumbia, A. Chériti

*Institut de recherche sur l'hydrogène, Département de génie électrique et génie informatique, Université du Québec à Trois-Rivières,
C.P. 500, Trois-Rivières, (QC), Canada G9A 5H7*

Received 21 April 2007; accepted 15 August 2007

Available online 22 October 2007

Abstract

In most of the maximum power point tracking (MPPT) methods described currently in the literature, the optimal operation point of the photovoltaic (PV) systems is estimated by linear approximations. However these approximations can lead to less than optimal operating conditions and hence reduce considerably the performances of the PV system. This paper proposes a new approach to determine the maximum power point (MPP) based on measurements of the open-circuit voltage of the PV modules, and a nonlinear expression for the optimal operating voltage is developed based on this open-circuit voltage. The approach is thus a combination of the nonlinear and perturbation and observation (P&O) methods. The experimental results show that the approach improves clearly the tracking efficiency of the maximum power available at the output of the PV modules. The new method reduces the oscillations around the MPP, and increases the average efficiency of the MPPT obtained. The new MPPT method will deliver more power to any generic load or energy storage media.

© 2007 Elsevier Ltd. All rights reserved.

Keywords: MPPT converter; MPPT method; Photovoltaic system; Nonlinear approach

1. Introduction

The operating power of photovoltaic (PV) modules depends on the sun's intensity, the ambient temperature and especially the PV modules' output voltage. If the transfer of power between PV source and load is not optimal, the total efficiency of the PV system will be affected negatively [1,2]. Several publications tackle the problem concerning the search of the optimal operating point by using various maximum power point tracking (MPPT) methods in order to extract the maximum energy from the PV modules. The majority of these first-class methods are based on so-called "hill-climbing" algorithms [3–5]. These methods can be used to determine the maximum power point (MPP) for specified sun radiation and temperature conditions; however they display oscillatory behaviour around the MPP under normal operating

conditions. Moreover, they can lead to a bad direction of the MPP tracking (i.e. towards less efficiency) in the case of a sudden variation of temperature and/or sun radiation when the system is already very near its actual MPP [6]. This is because the perturbation and observation (P&O) algorithm interprets the perturbation as the result of its previous variation of the array's operating voltage, and expects its next variation to be in the same direction as that of the previous one. These methods have the well-known drawback of causing corrections that, when the system is already operating at or very near its optimum power point, take it away from that position when a change in ambient conditions modify the output power of the PV modules. A second class of methods, based on look-up tables of the modules' characteristics, ought to be able to instantaneously determine the optimum point of operation when irradiation and/or temperature readings are available [7,8]; however the nonlinearity and the variation of the characteristics of the solar cells as a function of these variables make the establishment and the storage of a reliable look-up table rather difficult. A third class of

*Corresponding author. Tel.: +1 819 376 5011; fax: +1 819 376 5164.

E-mail address: kodjo.agbossou@uqtr.ca (K. Agbossou).

URL: <http://www.irh.uqtr.ca> (K. Agbossou).

methods, based on the mathematical modelling of the nonlinear current–voltage (I – V) characteristics of the PV modules, can be simple and able to quickly determine the optimal operation point of the PV system [9–12]. When using this modelling of the I – V characteristics method, the MPP is approximated for various conditions of load by a linear function of the short circuit current I_{sc} or of the open-circuit voltage V_{oc} . However that method has its own difficulties, as the proportion between optimal operating voltage and open-circuit voltage varies according to changing conditions of irradiation and temperature, and also that it is impossible to determine the V_{op} voltage by using only one linear function of the voltage V_{oc} [13].

This paper develops a nonlinear MPPT approach based on the measurement of the V_{oc} in order to read optimal operating conditions for the PV array. The combination of this approach with the usual P&O methods largely improves the performance of the MPP tracking of the PV systems. This new MPPT method is applicable to any kind of load connected to the PV array.

2. PV module characteristics

The equivalent electric diagram of a PV array is shown in Fig. 1. The PV array's electric characteristics under solar radiation is given in terms of output current I_{pv} and voltage V_{pv} [3,8]:

$$I_{pv} = I_L - I_O \left[\exp \left(\frac{V_{pv} + R_s I_{pv}}{V_T} \right) - 1 \right] - \frac{V_{pv} + R_s I_{pv}}{R_p}, \quad (1)$$

where $I_L = N_p I_{ph}$ corresponds to the light-generated current of the solar array with I_{ph} being the cell light-generated current and N_p represents the number of parallel modules.

$I_O = N_p I_{os}$ corresponds to the reverse-saturation current of the solar array, with I_{os} the cell reverse-saturation current.

$V_T = (N_s n K_B T) / q$ is the thermal voltage, where N_s is the number of cells connected in series, K_B the Boltzmann's constant, n the ideality factor, T the cell temperature, q the electron charge; R_s the series parasitic resistance of a solar array and R_p its shunt parasitic resistance. The load resistance is represented by R_{Load} .

The PV array's short-circuit current I_{sc} and open-circuit voltage V_{oc} at solar intensity G and cell temperature T

are given by [14]

$$I_{sc} = I_{sc}^* \left(\frac{G}{G^*} \right) + \alpha_1 (T - T^*), \quad (2)$$

$$V_{oc} = V_{oc}^* + \alpha_2 (T - T^*) - (I_{sc} - I_{sc}^*) R_s, \quad (3)$$

where I_{sc}^* and V_{oc}^* are the PV array short-circuit current and open-circuit voltage at the reference solar intensity G^* and the reference solar cell temperature T^* , and α_1 and α_2 are the solar cell temperature coefficients, respectively, for current and voltage.

An ideal PV module is one for which R_s is zero and R_p is infinitely large. The output current and voltage are then

$$I_{pv} = I_L - I_O \left[\exp \left(\frac{V_{pv}}{V_T} \right) - 1 \right], \quad (4)$$

$$V_{pv} = V_T \ln[(I_L - I_{pv}) / I_O + 1]. \quad (5)$$

The PV array characteristic presents three important points: the short circuit current I_{sc} , the open-circuit voltage V_{oc} and the optimum power P_{op} delivered by the PV array to an optimum load R_{op} when the PV modules operate at their MPP. Figs. 2(a) and (b) give the current–voltage (I – V) and power–voltage (P – V) characteristics of a PV module for different values of solar radiation and temperature. The short circuit current is clearly proportional to the solar radiation (Fig. 2(a)): more radiation, more current, and also more maximum output power. On the other hand the temperature dependence is inverse (Fig. 2(b)): an increase in temperature causes a reduction of the open-circuit voltage (when sufficiently high) and hence also of the maximum output power. Hence these opposite effects of the variations of solar radiation and temperature on the maximum output power make it important to track the MPP efficiently. The power curves of Fig. 2 show that the optimum power point corresponds to a load connected to the PV array that varies with the ambient conditions of illumination and temperature. In practice this variable optimal load will be achieved through the use of a variable duty cycle of the control part of the MPPT converter, which controls directly the operating voltage which corresponds to this optimal load.

3. MPPT converter configuration

Fig. 3 shows the MPPT buck converter diagram. The converter is composed of a power part and a control part. The switch S of the buck converter is a MOSFET transistor with a low internal resistance R_{on} . The MOSFET is controlled by a PWM signal generation circuit that uses a micro-controller. T is the period of the control signal and d is the duty cycle. The switch S is closed for the time dT and opened for the time $(1-d)T$ during each period [15]. In searching for the MPP and tracking this point in order to minimize the spread between the operating power and the

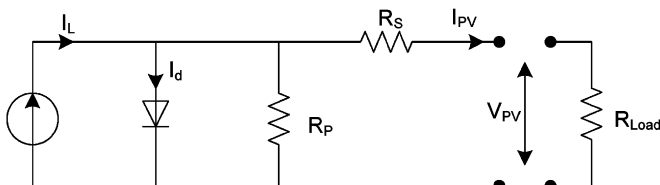


Fig. 1. Equivalent electric diagram of a solar array.

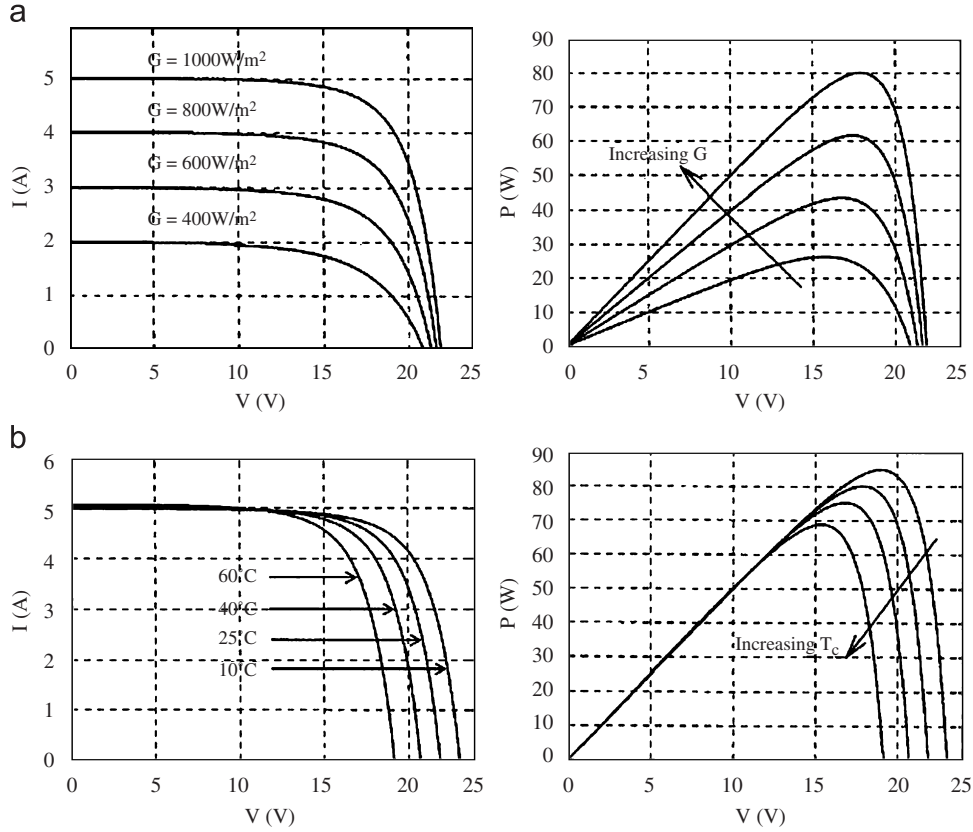


Fig. 2. Solar radiation and temperature influences on the I - V and P - V characteristics, (a) solar radiation influence, (b) temperature influence.

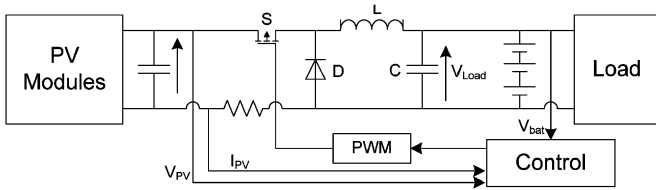


Fig. 3. MPPT buck converter diagram.

optimal power in the event of change of the weather conditions, the control circuit of the buck converter artificially perturbs periodically the operating point of the PV module. The resulting output voltage and current of the PV modules are then used by the control circuit to increase or decrease the duty cycle of the buck converter in order to change the operating point of the PV array. If the power is thereby increased, then the next perturbation will be in the same direction; otherwise the next perturbation will be in the opposite direction. The operation of the buck converter is characterized as follows:

When the transistor S is closed, the current in the inductance L grows from I_m to I_M and the voltage across the inductance is given by

$$V = V_{pv} - V_{Load} = L \frac{di}{dt} = \frac{(I_M - I_m)L}{t_{on}}. \quad (6)$$

When the transistor is opened, the voltage is

$$V = -V_{Load} = L \frac{di}{dt} = \frac{(I_m - I_M)L}{t_{off}}. \quad (7)$$

From Eqs. (6) and (7) we get

$$L(I_M - I_m) = (V_{pv} - V_{Load})t_{on} = V_{Load}t_{off}. \quad (8)$$

Hence

$$V_{pv}t_{on} = V_{Load}(t_{off} + t_{on}) = V_{Load}T \quad (9)$$

and thus

$$\frac{V_{Load}}{V_{pv}} = \frac{t_{on}}{T} = d. \quad (10)$$

If the converter's losses are negligible, its power transfer equation becomes

$$V_{pv}I_{pv} = V_{Load}I_{Load} \quad (11)$$

and that gives

$$\frac{V_{Load}}{V_{pv}} = \frac{I_{pv}}{I_{Load}} = \frac{t_{on}}{T} = d. \quad (12)$$

For each value of load resistance $R_{Load} = V_{Load}/I_{Load}$, it is thus possible to define a corresponding value of converter input resistance R_e :

$$R_e = \frac{V_{pv}}{I_{pv}} = \frac{(V_{Load}/d)}{I_{Load}d} = \frac{V_{Load}}{I_{Load}d^2} = \frac{R_{Load}}{d^2}. \quad (13)$$

To adapt the load R_{Load} to the PV modules and extract the maximum power from them, the duty cycle is set to its optimal value d_{op} which corresponds to the optimal operating point (V_{op} , I_{op}), see Fig. 4.

4. MPP search analysis

The variable load required to produce maximum power as a function of varying conditions of illumination and

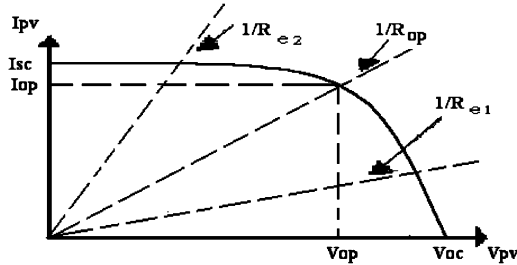


Fig. 4. PV system operating points variation with load change.

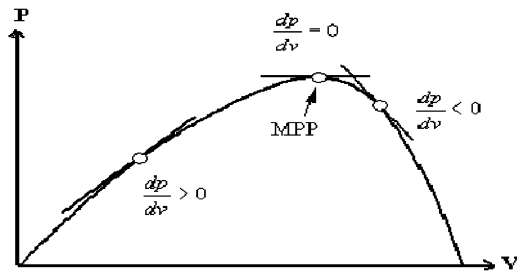


Fig. 5. Possible displacements of the operating point.

temperature will be the input resistance of the converter. When the solar radiation and temperature varied as shown in Fig. 2, each of the MPPs corresponds to only one value of the input resistance of the converter. Then when the solar radiation or temperature changes, the value of input resistance seen by solar modules must be changed to locate the new MPP, and this will be achieved by varying the duty cycle.

In past years, the MPPT methods proposed resulted in oscillations of the position of the MPP which can actually lead it away from its optimal value [6]. In order to overcome this drawback, an analysis is provided to understand the expected displacement of the operating point resulting from an applied perturbation of the operating conditions. Fig. 5 presents a typical curve of PV power variation according to the operating voltage. This figure shows that there are two operating zones: the first is located on the right side of the MPP where $dP/dV < 0$ and the second on the left side of the MPP where $dP/dV > 0$.

Four cases of perturbations from the operating point can be distinguished:

First case: (Fig. 6(a)): After the perturbation, there is a displacement of the operating point from $k-1$ to k , with $P(k) > P(k-1)$ and $V(k) > V(k-1)$. The power increases after the perturbation. This indicates that the MPP search is oriented in the right direction. The search of the MPP continues in the same direction and reaches the operating point $k+1$ by increasing the duty cycle by Δd . The voltage is then increased to $V(k+1) = V(k) + \Delta v$.

Second case: (Fig. 6(b)): After the perturbation, there is a displacement of the operating point from $k-1$ to k , with $P(k) < P(k-1)$ and $V(k) < V(k-1)$. The power decreases after the perturbation. This indicates that the MPP search is oriented in the wrong direction. The MPP search

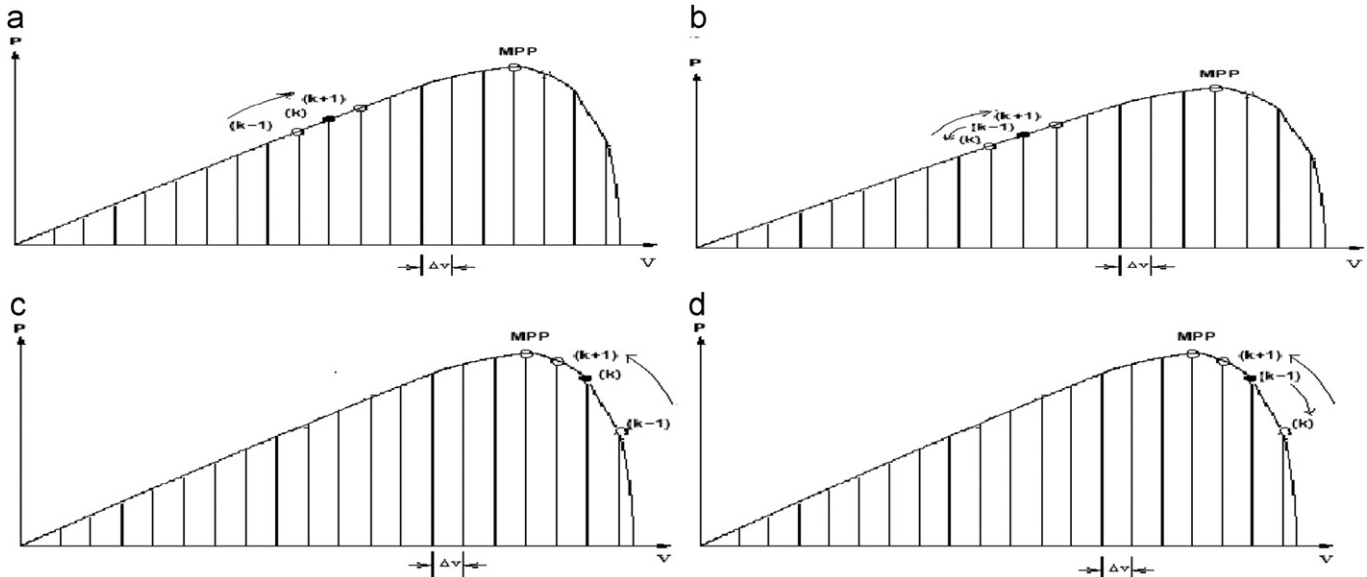


Fig. 6. Various cases of displacement of the operating point, (a) first case of operation, (b) second case of operation, (c) third case of operation and (d) fourth case of operation.

Table 1
Summary of control action for various operating points

Case	ΔV	ΔP	$\frac{\Delta P}{\Delta V}$	Tracking direction	d : Duty cycle control action
1	+	+	+	Good direction	Increase $d(k) = d(k-1) + \Delta d$
2	-	-	+	Bad direction	Increase $d(k) = d(k-1) + 2\Delta d$
3	-	+	-	Good direction	Decrease $d(k) = d(k-1) - \Delta d$
4	+	-	-	Bad direction	Decrease $d(k) = d(k-1) - 2\Delta d$

direction must be changed and the duty cycle is increased by $2\Delta d$ to reach the operating point $k+1$. The voltage is then increased to $V(k+1) = V(k) + 2\Delta v$.

Third case: (Fig. 6(c)): After the perturbation, there is a displacement of the operating point from $k-1$ to k so that $P(k) > P(k-1)$ and $V(k) < V(k-1)$. The power increases after perturbation. This indicates that the MPP search is oriented to the good direction. Then, the MPP search direction must be maintained and the duty cycle is decreased by Δd to reach the operating point $k+1$. The voltage is then decreased to $V(k+1) = V(k) - \Delta v$.

Fourth case: (Fig. 6(d)): After the perturbation, there is a displacement of the operating point from $k-1$ to k so that $P(k) < P(k-1)$ and $V(k) > V(k-1)$. The power decreased. This indicates that the MPP search is oriented to bad direction. The MPP search direction must be changed and the duty cycle is increased by $2\Delta d$ to reach the operating point $k+1$. The voltage is then decreased to $V(k+1) = V(k) - 2\Delta v$.

The search rules for the four cases of operation are summarized in Table 1. Clearly cases 1 and 3 proceed in the correct direction, whereas cases 2 and 4 must reverse direction.

5. New MPPT method for PV systems

5.1. Current-based and voltage-based MPPT

To determine the optimal operating point corresponding to the maximum power for the various levels of solar radiation and temperature, numerical methods can be used to show the linear dependence between the optimal current and the short circuit current [9,10,13]. The basic equation can be given as

$$I_{op} = K_i I_{sc}, \quad (14)$$

where K_i is the current proportionality constant.

This equation characterizes the key idea of the technique called current-based MPPT (CMPPT). A similar approach, based on the linear approximation of the optimal voltage relative to the open-circuit voltage, can also be used to determine the MPP [11,12]. Eq. (15) represents this concept of technique called voltage-based MPPT (VMPPT):

$$V_{op} = K_v V_{oc}, \quad (15)$$

where K_v is the voltage proportionality constant.

Both types of MPPT methods may be used either with buck or boost converters, depending on the load characteristics. The short-circuit current depends linearly on the solar irradiation, while the open-circuit voltage depends logarithmically on the solar irradiation [16,17]. The studies tend to show that the linear approximation of the current used in the CMPPT technique is more accurate when compared with the linear approximation of the voltage used in the VMPPT technique. However, the technique of VMPPT is more effective and has less loss (particularly for MPPT buck converters). In addition, online measurements of PV short-circuit current and output currents make CMPPT hardware more complex compared (same rating) with VMPPT circuitry that requires voltage measurement only [10]. From this analysis, a novel nonlinear approach of the MPP value estimation is proposed.

5.2. New MPPT method

The approach is based on the open-circuit voltage measurement and a nonlinear calculation of the optimal voltage. Maximum power $P_{op} = V_{op} I_{op}$, is obtained by canceling the derivative of the power:

$$\left(\frac{dP}{dI_{pv}} \right) = \frac{d(V_{pv} I_{pv})}{dI_{pv}} = 0, \quad (16)$$

which leads to

$$\left(\frac{dV_{pv}}{dI_{pv}} \right)_{op} = - \frac{V_{op}}{I_{op}}. \quad (17)$$

The derivative of the relation (5) put into (17) gives

$$\frac{V_{op}}{I_{op}} = - \frac{V_T}{(I_{sc} + I_O - I_{op})}. \quad (18)$$

Taking into account Eq. (14), V_{op} can be found as

$$V_{op} = \frac{V_T I_{op}}{\left(1 - \frac{1}{K_i}\right) I_{op} - I_O}. \quad (19)$$

The open-circuit voltage of the PV modules is given by

$$V_{oc} = V_T \ln \left[\frac{I_{sc}}{I_O} + 1 \right]. \quad (20)$$

The I_{op} is deduced from Eqs. (17) and (19):

$$I_{op} = K I_O \left[\exp \left(\frac{V_{oc}}{V_T} \right) - 1 \right]. \quad (21)$$

The optimal voltage can be calculated from Eqs. (19) and (21):

$$V_{op} = \frac{V_T [\exp(V_{oc}/V_T) - 1]}{(1 - 1/K) \exp(V_{oc}/V_T) - 1}. \quad (22)$$

Fig. 7 gives the algorithm of the method based on this nonlinear approach. To estimate the MPP reference value, the open-circuit voltage of the PV modules is measured cyclically at the output solar panels during the opening of the switch of the buck converter. This voltage allows the MPP reference value to be calculated from Eq. (22), and

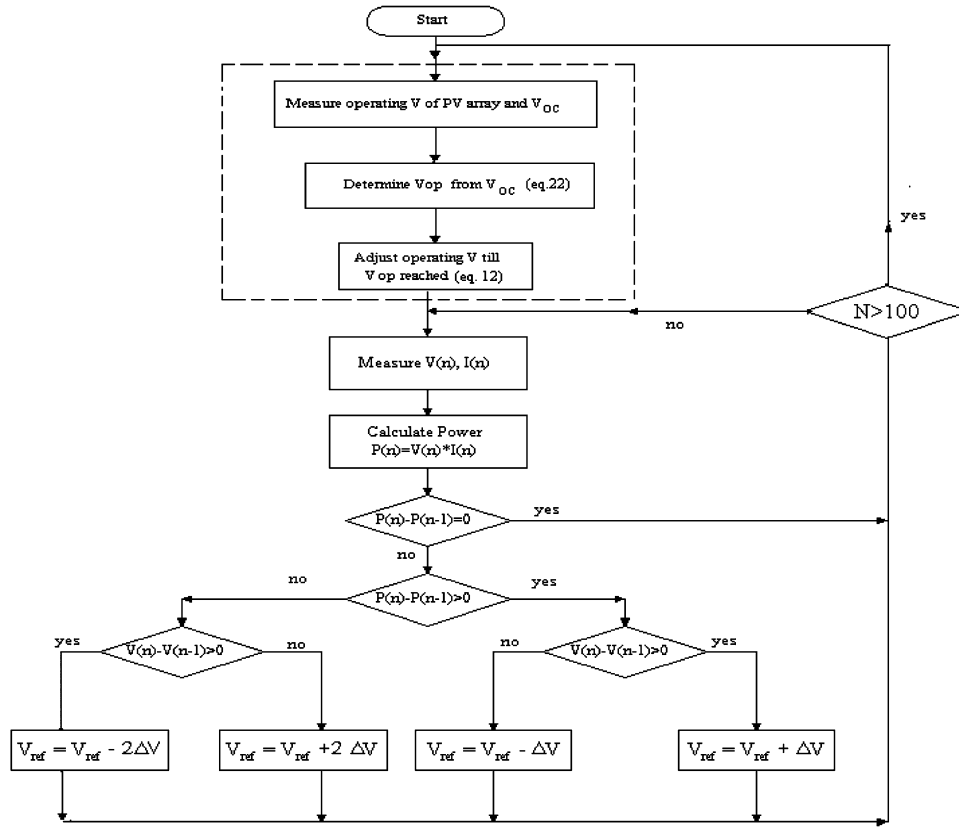


Fig. 7. Algorithm of the P&O method with cyclic measurement of the tracking reference.

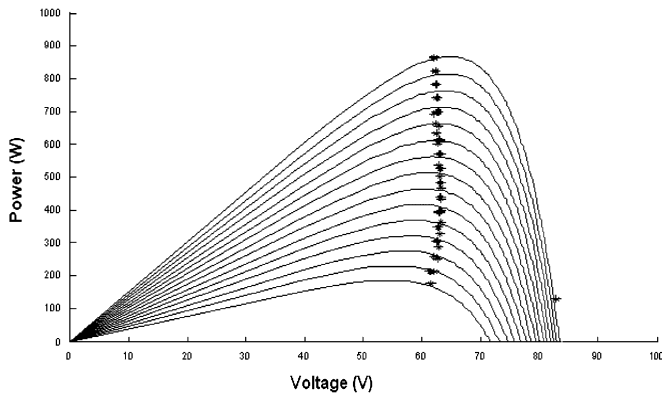


Fig. 8. Proposed tracking methods for power versus voltage.

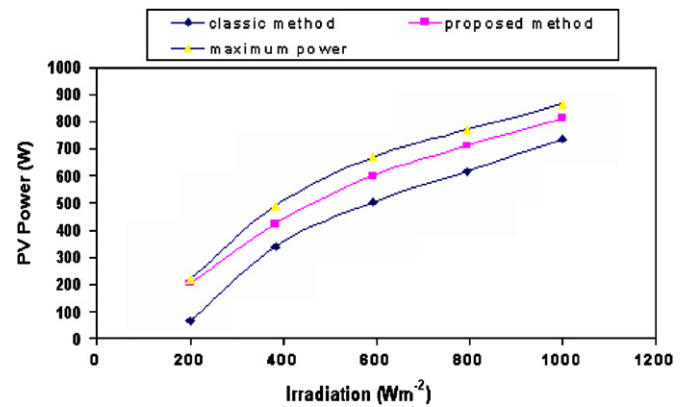


Fig. 9. Available output power of the PV modules.

consequently the value of the converter's duty cycle to be adjusted by using Eq. (12).

The proposed algorithm and the classic P&O methods were compared by simulations using Matlab. The simulation results are shown in Figs. 8–10. The solar irradiance profile is supposed to be growing linearly. With the proposed MPPT approach (Fig. 8), the oscillations around the MPP are almost completely eliminated. Fig. 9 shows the available output power of the PV modules when using the proposed method and the classical method. The maximum power and solar irradiation are taken from the

characteristics of the installed PV array provided by the manufacturer (model GP-64 “Golden Genesis”).

To validate the proposed MPPT algorithm, a comparison is done between the classic P&O algorithm and the above proposed method. The comparison was based on the tracking efficiency of the maximum power available at the solar panels. The tracking efficiency is defined as [6]

$$\eta_T = \frac{1}{n} \sum_{i=1}^n \frac{P_i}{P_{\max,i}}, \quad (23)$$

where P_i represents the PV modules' output power, $P_{\max,i}$ represents the maximum power available at the PV modules and n is the number of samples.

The tracking efficiency of the proposed method is an average of 92% compared to 68% for the classical P&O method (Fig. 10).

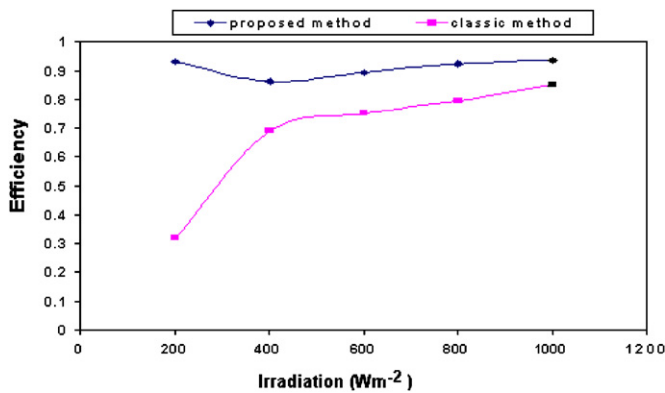


Fig. 10. Tracking efficiency.

6. Experimental set-up and results

The experimental tests were carried out on the test bench of the stand-alone renewable energy system installed at the Hydrogen Research Institute [1]. The test bench includes a 1 kW solar panel, a 10 kW wind turbine, a 5 kW electrolyser, a compressor, a storage tank, a 5 kW fuel cell, a 48 V DC bus, a DC/AC converter (48–120 V/60 Hz), power interfaces and a control system [15]. The PV array has been used for charging the battery bank, which will work as buffer energy storage for the system. The excess energy is stored in the batteries for short term and stored in the form of hydrogen for long term. The use of the MPPT method increases the produced energy by PV arrays, thus increasing the available energy for hydrogen production.

Figs. 11 and 12 give the experimental results obtained, respectively, with the classic P&O method and with the proposed nonlinear approach. Voltage, current, duty cycle and the PV output power are plotted versus running time. The MPPT control methods were implemented in a circuit

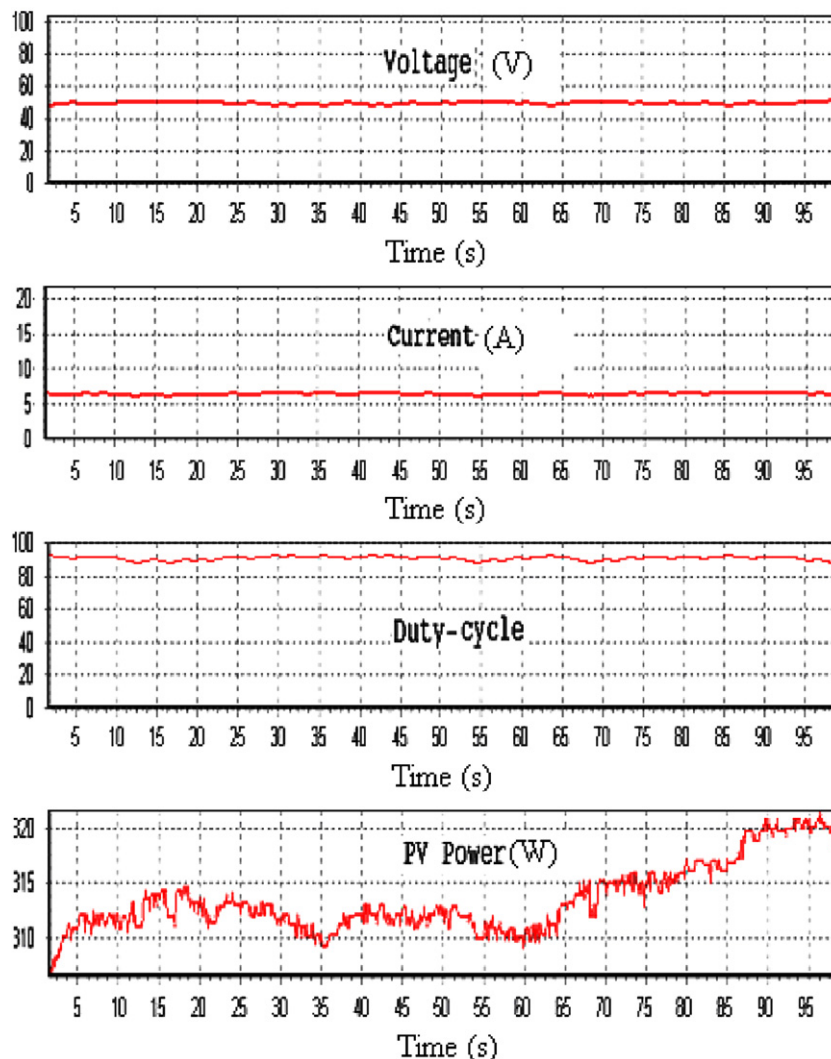


Fig. 11. Experimental results of the P&O method.

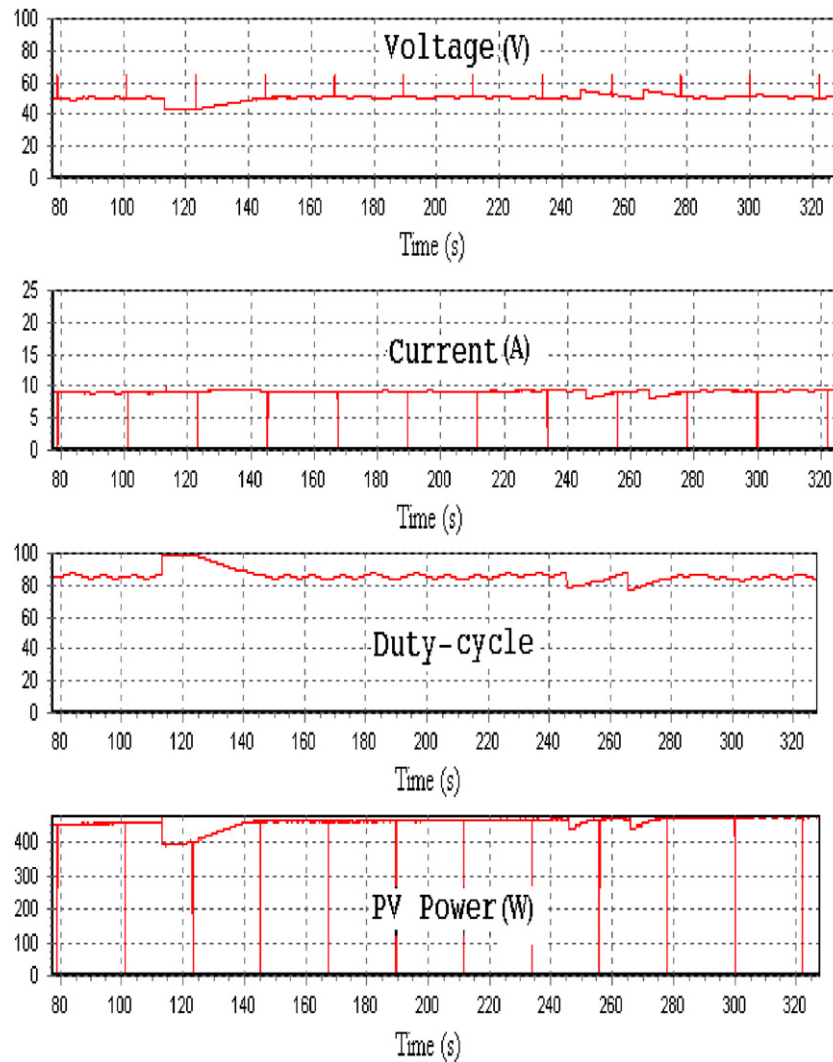


Fig. 12. Experimental results of the nonlinear method.

based on a micro-controller PIC18F242. Normally the duty cycle values are zero during the measurement of the open-circuit voltage, but due to the refreshing period of the micro-controller memory, the zero crossing of the duty cycle is not plotted. The open-circuit voltage sampling time can be chosen with different sampling values, but it is important that this time be much lower than the open-circuit period. When the classic P&O method is implemented, it does not instantly locate the MPP and it has also an oscillation around the MPP. This instability is particular to the P&O algorithm alone. On the other hand the method based on the nonlinear approach converges quickly by positioning the search directly on the MPP, with no discernable oscillations. The tracking efficiency is improved on average by 17%. The observed spikes on the PV voltage and PV current are due to the periodic openings of the MOSFET controller (every 20 s—Fig. 12) to permit the measurements of the open-circuit voltage to determine the MPP tracking reference.

7. Conclusion

A new MPPT method based on a nonlinear approach for estimating the optimal operating point was developed. Using this method, it is possible to adapt the load to the PV modules and to follow the MPP howsoever the weather conditions may vary. Experimental results of this new approach showed that the tracking efficiency of the MPP is better than that obtained with the classic P&O method. The new nonlinear method produced practically no oscillations around the MPP, the main weakness of the P&O method. Implementation of such a method in PV systems will increase the power delivered to any generic load or energy storage media. The experimental results were obtained with the IRH test bench of the stand-alone renewable energy system based on hydrogen storage. The results show that the gain in power obtained by this new method can clearly increase the hydrogen production and storage rates from PV systems because of the improved

control of the MPP during changing ambient weather conditions.

Acknowledgements

This work has been supported by the LTE Hydro-Québec, Natural Resources Canada and the Natural Sciences and Engineering Research Council of Canada.

References

- [1] Agbossou K, Kolhe M, Hamelin J, Bose TK. Performance of stand-alone renewable energy system based on energy storage as hydrogen. *IEEE Trans Energy Convers* 2004;19:633–40.
- [2] Applebaum J. The quality of load in a direct-coupling photovoltaic system. *IEEE Trans Energy Convers* 1987;2(4):534–41.
- [3] Koutroulis E, Kalaitzakis K, Voulgaris NC. Development of a micro-controller based photovoltaic maximum power point tracking control system. *IEEE Trans Power Electron* 2001;16:46–54.
- [4] Hua C, Lin J, Shen C. Implementation of a DSP-controlled photovoltaic system with peak power tracking. *IEEE Trans Ind Electron* 1998;45:99–107.
- [5] Chiang J, Chang KT, Yen CY. Residential photovoltaic energy storage system. *IEEE Trans Ind Electron* 1998;45:385–94.
- [6] Hohm DP, Ropp ME. Comparative study of maximum power point tracking algorithms using an experimental, programmable, maximum power point tracking test bed. In: *Proceedings of the 28th IEEE photovoltaic specialists conference*, 2000. p. 1699–1702.
- [7] Yamashita H, Tamahashi K, Michihira M, Tsuyoshi A, Amako K, Park M. A novel simulation technique of the PV generation system using real weather conditions. In: *Proceedings of the power conversion conference, PCC, Osaka, 2002*, vol. 2. p. 839–44.
- [8] Park M, Yu IK. A novel real-time simulation technique of photovoltaic generation systems using RTDS. *IEEE Trans Energy Convers* 2004;19:164–9.
- [9] Alghuwainem SM. Matching of a DC motor to a photovoltaic generator using a step-up converter with a current-locked loop. *IEEE Trans Energy Convers* 1994;9:192–8.
- [10] Masoum MAS, Dehbonei H, Fuchs EF. Theoretical and experimental analyses of photovoltaic systems with voltage and current-based maximum power-point tracking. *IEEE Trans Energy Convers* 2002;17:514–22.
- [11] Enslin JHR, Wolf MS, Snyman DB, Swiegers W. Integrated photovoltaic maximum power point tracking converter. *IEEE Trans Energy Convers* 1997;44:769–73.
- [12] Masoum MAS, Badejani SMM, Fuchs EF. Microprocessor-controlled new class of optimal battery chargers for photovoltaic applications. *IEEE Trans Energy Convers* 2004;19:599–606.
- [13] Noguchi T, Togachi S, Nakamoto R. Short-current pulse-based maximum-power-point tracking method for multiple photovoltaic-and-converter module system. *IEEE Trans Ind Electron* 2002;49:217–23.
- [14] Anna Fay W. *The handbook of photovoltaic applications: building applications and system design considerations*. Atlanta, Georgia: Fairmont Press; 1986.
- [15] Tafticht T, Agbossou K. MPPT method development for photovoltaic systems. In: *Proceedings of the IEEE Canadian conference on electrical and computer engineering, CCGEI 2004*, Niagara Falls, Ontario 2004.
- [16] Appelbaum J. Discussion of theoretical and experimental analyses of photovoltaic systems with voltage and current-based maximum power point tracking. *IEEE Trans Energy Convers* 2004;19:651–2.
- [17] Akbaba M. Matching three-phase AC loads to PVG for maximum power transfer using an enhanced version of the Akbaba model and double step-up converter. *Sol Energy* 2003;75(1):17–25.